Composite Structures 319 (2023) 117081

Contents lists available at ScienceDirect

Composite Structures

journal homepage: www.elsevier.com/locate/compstruct

# A new model for predicting the shear strength of RC beams strengthened with externally bonded FRP sheets

Amirhossein Mohammadi [a,*], Joaquim A.O. Barros [b], José Sena-Cruz [b]

[a] University of Minho, ISISE, ARISE, Department of Civil Engineering, 4800-058 Guimarães, Portugal
[b] University of Minho, ISISE, ARISE, IBS, Department of Civil Engineering, 4800-058 Guimarães, Portugal

ARTICLE INFO

*Keywords:*
Analytical model
Shear strengthening
Reinforced concrete beams
Externally bonded
FRP
Design guidelines

ABSTRACT

Externally bonded fibre reinforced polymer (FRP) reinforcements have been widely used for upgrading the shear resistance of reinforced concrete (RC) structures. This technique has been widely studied and numerous analytical models currently exist to predict the contribution of FRP for the shear resistance of RC beams. In this study, some of the most well-known models recommended in guidelines (including *fib* bulletin 90, CNR-DT 200 R1/2013, and ACI 440.2R-17) are selected, and their predictive performance are assessed using a large database of 344 beams compiled from published works. In addition, this study introduces a novel model that accounts for a missing influential predictive component in the existing models, namely the ratio of existing steel stirrups. The comparison of the results obtained with this model and those from the current models demonstrates the best predictive performance of the new one.

## 1. Introduction

Reinforced concrete (RC) structures have been widely built over the past several decades. However, these structures may fail to meet the nowadays requirements of design codes and need strengthening [1]. Degradation of mechanical properties [2,3] (due to environmental condition, accidents, etc.) and increase in the demanded load capacity caused by increase in seismic or service loads [4-6] are some of the common reasons of widespread use of strengthening techniques. RC beams are one of the prevalent elements in RC structures that require (flexural and/or shear) strengthening [7-10]. Shear failure in the RC beams is brittle and occurs suddenly, generally causing large damages. In the past three decades, fibre reinforced polymer (FRP) materials have been extensively used as Externally Bonded Reinforcement (EBR) to increase the shear resistance of RC beams. To date, many empirical, conceptual, and numerical models have been developed to predict the shear capacity of these beams; nonetheless, this task remains challenging. Due to its simplicity, most design guidelines use a conventional truss model to evaluate the contribution of FRP reinforcement, analogous to the one used to predict the contribution of steel stirrups [11-13].

Like in the steel shear reinforcement, some models assume the strain mobilized in FRP at the failure of a shear strengthened RC beam (currently designated by effective strain) is a constant value [14-16]. However, it has been demonstrated by many researchers that this effective strain is not constant and depends on some variables. In 1998, Triantafillou [17] was among the first researchers to propose a model with a varying effective strain for FRP reinforcement as a function of the axial stiffness of FRP reinforcement ($\rho_f E_f$). This model was later modified by Triantafillou and Antonopoulos [18] in 2000 and was adopted by *fib* bulletin 14 [19]. The continuous research has shown that the effective strain of FRP shear reinforcements also depends on the beam's cross-section corners where FRP is installed [20] and concrete substrate quality [21,22]. It was verified that the bond strength and ductility between FRP and concrete substrate decrease with the quality of the concrete substrate, generally correlated with the concrete compressive strength, resulting premature debonding with smaller FRP effective strain. The FRP bond length is another important variable discussed in the literature, since below what is designated as effective bond length (length above which the maximum bond force is not exceeded), the maximum strain capable to be mobilized decreases with the bond length [22-24]. The shear span to effective depth ratio was also shown affecting the FRP effective strain [21,25]. It was observed that at the failure of a beam shear strengthened with a relatively high FRP reinforcement ratio, existing steel stirrups might not reach the yielding strain, therefore their shear strengthening potential is not fully mobilized [26-29]. Furthermore, it was shown that the crack inclination angle is not a constant value [30-33], which has a significant influence on the FRP shear

* Corresponding author.
*E-mail addresses:* amir.xdbx@gmail.com (A. Mohammadi), barros@civil.uminho.pt (J.A.O. Barros), jsena@civil.uminho.pt (J. Sena-Cruz).

https://doi.org/10.1016/j.compstruct.2023.117081
Received 12 January 2023; Received in revised form 7 March 2023; Accepted 22 April 2023
Available online 30 April 2023

**Nomenclature**

| | |
|---|---|
| $A_{fwc}$ | Effective FRP cross-section area (mm$^2$) |
| $a_t$ | Reduction factor to account for the long-term effects |
| $b_w$ | Width of the beam's web (mm) |
| $\boldsymbol{C}$:$p \times p$ symmetrical covariance matrix | symmetrical covariance matrix |
| $CoV$ | Coefficient of variation |
| $d$ | Effective depth of the beam (mm) |
| $d_i$ | Mahalanobis distance of $i^{\text{th}}$ observation |
| $d_{fv}$ | Effective depth of FRP (mm) |
| $E_f$ | Elastic modulus of FRP (MPa) |
| $E_f t_f$ | Axial stiffness of FRP (N/mm) |
| $f_{cm}$ | Concrete mean compressive strength (MPa) |
| $f_{fe}$ | Effective stress in the FRP reinforcement (MPa) |
| $f_{fw,c}$ | FRP strength attributed to a failure caused by FRP rupture (MPa) |
| $f_{fbw}$ | Bond strength of FRP reinforcement (MPa) |
| $f_{fbk}$ | FRP debonding strength according to *fib* bulletin 90 (MPa) |
| $f_{fee}$ | FRP debonding stress according to CNR-DT 200.R1-2013 (MPa) |
| $h$ | Height of the beam (mm) |
| $h_f$ | Height of FRP (mm) |
| $h_{fe}$ | Effective height of FRP (mm) |
| $h_w$ | Height of the beam's web (mm) |
| $k_b$ *and* $k_G$ | Empirical coefficients |
| $l_{ed}$ | Effective bond length (mm) |
| $l_e$ | Effective bond length of FRP (mm) |
| $MAPE$ | Mean absolute percentage error |
| $m_F$ | Modification factor |
| $n_f$ | Number of FRP layers |
| $p$ | Number of variables |
| $Q_1$ | Lower quartile |
| $Q_3$ | Upper quartile |
| $R$ | Radius at the corner of the beam's cross-section (mm) |
| $R^2$ | Absolute Fraction of Variance |
| $r$ | Pearson coefficient of correlation |
| $RMSE$ | Root mean squared error (kN) |
| $s_f$ | Spacing of FRP strips (mm) |
| $s_{0k}$ | Characteristic ultimate deformation capacity (mm) |
| $SD$ | Standard deviation |
| $t_{fe}$ | Effective thickness of FRP (mm) |
| $t_f$ | Thickness of one layer of FRP (mm) |
| $V_{R,f}^{\exp}$ | Shear contribution of FRP according to experimental results (kN) |
| $V_R^{ref}$ | Overall shear strength of the reference beam (kN) |
| $V_R^{str}$ | Overall shear strength of the strengthened beam (kN) |
| $V_{R,f}^{mod\ el}$ | Nominal shear contribution of FRP predicted by each model (kN) |
| $V_{R,c}$ | Shear contribution of concrete (kN) |
| $V_{R,s}$ | Shear contribution of transversal steel (kN) |
| $V_{R,f}$ | Shear contribution of FRP reinforcement (kN) |
| $V_{R,\max}$ | Shear strength of concrete compression strut (kN) |
| $w_f$ | Width of FRP strips (mm) |
| $\boldsymbol{X}$ | Matrix of n observations of p variables |
| $\boldsymbol{x}_i$ | Vector of variables for the $i^{\text{th}}$ observation |
| $\alpha$ | Inclination of FRP fibres |
| $\varepsilon_{fe}$ | Effective strain in the FRP composite |
| $\varepsilon_{fu}$ | Strain at the failure of the FRP coupon |
| $\theta$ | Crack inclination angle |
| $\kappa_R$ | Modification factor accounting for the stress distribution in the FRP |
| $\kappa_1$ | Modification factor that accounts for the quality of the concrete substrate |
| $\kappa_2$ | Modification factor accounting for the bond mechanism |
| $\boldsymbol{\mu}$ | Vector of mean values for p variables |
| $\rho_{sw}$ | Stirrup ratio (%) |
| $\rho_{sl}$ | Longitudinal steel ratio (%) |
| $\tau_{b1k}$ | Characteristic ultimate bond strength |
| $\chi$ | Model error |

contribution. However, the prediction of this variable is still not straightforward.

There are already models that account for the most influential variables. For instance, in 2012 Chen et al. [28] proposed an analytical model that can predict the shear contribution of FRP with high accuracy. In addition, they proposed a modification factor to account for the negative effect of interaction between internal steel stirrups and external FRP shear reinforcement, hence increasing the predictive performance of the model. However, these types of models require knowledge of a broader set of parameters to solve the equations, making their use for design purposes difficult, if not impossible. In addition, the application of the Modified Compression Field Theory (MCFT) [34] may also improve the predictive performance since the formulation integrates the evaluation of the crack inclination angle. Due to the iterative procedure of MCFT equations, more complexity is introduced, making these models less practical from a design standpoint. These models are rarely adopted in the current design guidelines. The models adopted in the design guidelines are straightforward and practical, yet they produce less accurate predictions. This may be due to the fact that these models exclude some influential variables, such as the reinforcing ratio of steel stirrup.

In this work, a large dataset composed of 344 experimental results of beams shear strengthened with the EBR technique is collected from the published literature. Based on this data, the predictive performance of some well-known recent models is evaluated, and a new model is proposed. The results show that the accuracy of the proposed model has outperformed current models, yet the procedure is practical for its use in design practice. Given the fact that some guidelines do not include equations for the side-bonded configuration due to its lower efficiency, this research focuses exclusively on beams strengthened by either fully wrapped or U-wrapped beams.

## 2. Construction of the dataset

A comprehensive database of over 900 tested RC beams that are transversely reinforced with FRP materials was compiled [35]. This database includes detailed information on test specimens such as geometry (e.g., the length, cross-section, test set-up), material properties (e.g., the concrete compressive strength and the mechanical properties of flexural and shear reinforcement), FRP and conventional steel reinforcements details, and test results (e.g., shear capacity before and after strengthening with FRP, and failure mode). Due to the diverse range of experiments included in this dataset, the updated version of the database that contains 383 specimens excluded those that displayed any of the following characteristics: (1) specimens with missing data that are required for the analysis; (2) specimens where the FRP were not in carbon fibres (CFRP); (3) specimens reinforced with the NSM technique; (4) specimens with a negligible shear contribution of FRP for the shear resistance $V_f^{\exp} < 10$ kN (suspicion of some incorrection on the strengthening process); (5) specimens with two-sided FRP

reinforcement (as this technique is not considered in some guidelines, such is the case of *fib* bulletin 90); (6) specimens that are strengthened with FRP systems with multidirectional fibres, e.g. fabrics; (7) and, specimens with any kind of end anchorage (since the effectiveness is too dependent of the type of anchorage adopted).

### 2.1. Outlier detection

The eventual existence of outliers in the compiled dataset was checked, i.e., data points that deviate significantly from normal data, which may influence, detrimentally, the model's predictive performance. Outliers exist due to several factors, such as data entry or measurement errors, sampling problems and unusual conditions, and natural variation. Univariate methods are often used to detect the outliers. Although these methods are easy to implement, they may fail to detect an outlier in multivariable data. In this study selected predictive variables and the contribution of FRP to shear resistance of the beam form a multivariate space. This study employs Mahalanobis Distance (MD) Method, an effective approach for [36] detecting outliers in multivariate space. The MD is a useful multivariate distance metric to evaluate the distance between a single data point and a distribution, which can be found as follow:

$$d_i^2 = (\boldsymbol{x}_i - \boldsymbol{\mu})^T (\boldsymbol{C}^{-1})(\boldsymbol{x}_i - \boldsymbol{\mu})$$

$$\boldsymbol{x}_i = \{\boldsymbol{x}_i^1, \ldots, \boldsymbol{x}_i^p\};\ \mu_i = \{\boldsymbol{\mu}_i^1, \ldots, \boldsymbol{\mu}_i^p\};\ \boldsymbol{C} = \begin{bmatrix} VAR(\boldsymbol{x}_i^1) & \cdots & Cov(\boldsymbol{x}_i^1, \boldsymbol{x}_i^p) \\ \vdots & \ddots & \vdots \\ Cov(\boldsymbol{x}_i^p, \boldsymbol{x}_i^i) & \cdots & VAR(\boldsymbol{x}_i^p) \end{bmatrix} \quad (1)$$

In this equation, $d_i$ is the Mahalanobis distance of observation $i$; $\boldsymbol{x}_i$ is a vector of $p$ variables representing the $n$ observations ($i = 1,2,\ldots,n$); $\boldsymbol{\mu}$ is the vector of mean values for $p$ variables, and C is $p \times p$ symmetrical covariance matrix. According to the proposed model presented later, $\boldsymbol{x}_i$ consists of the predictive and target variables as follow:

$$\boldsymbol{x}_i = \left\{ \left(E_f \rho_f / f_{cm}^{2/3}\right)_i, \rho_{sw_i}, \rho_{sl}, \varepsilon_{fe_i} \right\} \quad (2)$$

where $E_f\rho_f/f_{cm}^{2/3}$ is the normalized axial stiffness; $\rho_{sw} = A_{sw}/(b_w s_s)$, $\rho_{sl} = A_{sl}/(b_w d_s)$ and $\rho_f$ are the reinforcing ratio of steel stirrups, the reinforcing ratio of tensile steel reinforcement, and the strengthening ratio of FRP reinforcement (later will be defined), respectively. In Eq. (1), $\varepsilon_{fe}$ is the effective strain of FRP as defined later in Eq. (30) and $E_f$ is the elastic modulus of FRP, while $f_{cm}$ is the mean concrete compressive strength.

If the $d^2$ follows a chi-square distribution, a critical value for $d^2$ to recognize an specimen as an outlier is determined using a significance level of 0.05 (as there is four degrees of freedom, which is equal to the number of variables in the $x_i$ vector, the critical value of 9.49 is determined). Specimens with $d^2$ higher than the chi-square critical value will be considered outliers. The $d^2$ for each specimen is depicted in Fig. 1, where outliers were shown in red colour (10% of the initial total updated dataset). The remaining 344 specimens [9,20,32,33,37–100,110,111] are used for developing a new model, as well as to validate both this model and existing models.

### 2.2. Statistical characteristics of some important variables

The model developed in this study should be applied with caution to specimens whose variables fall outside the range examined in this study, as generalization beyond this range may result in inaccurate results. The statistical characteristics of some important variables are given in Table 1.

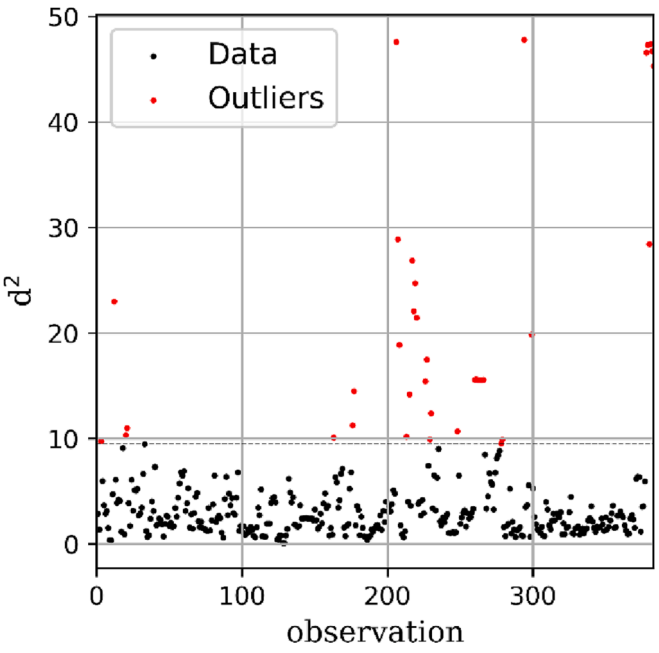


**Fig. 1.** Outlier detected using Mahalanobis Distance Method.

## 3. Review of the current design provisions for the contribution of externally bonded FRP shear reinforcement

Although it is known that there is a certain interdependency between the shear strength contributions provided by concrete, stirrups, and FRP [28,29,101], the superposition principle is generally used in the models proposed in the guidelines. The shear contribution of FRP is, therefore, calculated independently and added to the other contributions [102-105]. The overall shear resistance is then expressed as:

$$V_R = V_{R,c} + V_{R,s} + V_{R,f} \leqslant V_{R,\max} \quad (3)$$

where $V_{R,c}$, $V_{R,s}$ and $V_{R,f}$ are the shear contribution of concrete, steel stirrups and FRP reinforcement, respectively, while $V_{R,max}$ is the shear strength provided by the concrete crushing of the compressive strut formed at beam's failure.

The guideline models utilize truss analogy and propose similar equations for finding the FRP contribution. Their principal difference is how to calculate the effective strain or stress in the FRP composite ($\varepsilon_{fe}$ or $f_{fe}$) at beam's shear failure. The predictive performance of some of the most renowned models is evaluated in this study, including *fib*-Bulletin 90 [12], CNR-DT200 [13], and ACI 440-2R [11]. In the following section, the equations used to calculate the shear contribution of FRP in accordance with the aforementioned design guidelines are concisely presented.

### 3.1. fib-bulletin 90 (fib-TG5.1)

The *fib* TG5.1 [12] has proposed a model that can be used for fully (O configuration) or U-wrapped beams.

$$V_{R,f} = A_{fwc} h_{fe} f_{fe} (\cot\theta + \cot\alpha_f) \sin\alpha_f \quad (4)$$

where $A_{fwc}$ is the effective FRP cross-section area calculated as $2w_f t_{fe}/s_f$ for strips and $2t_{fe}sin\alpha_f$ for continuous FRP sheets, being $w_f$, $t_{fe}$ and $s_f$ the width, the effective thickness and the spacing of FRP strips, and $\alpha_f$ the angle between the longitudinal axis of the beam and the fibres of these strips, as depicted Fig. 2. In Eq. (4) $h_{fe}$ is the effective height of FRP calculated as a minimum of $h_f$ and $h - 0.1d_s$, where $h_f$, $h$, and $d_s$ stand for the height of FRP, the height of the beam's cross section and the effective depth of the beam's longitudinal tensile steel reinforcement,

**Table 1**
Statistical summary of some crucial variables for strengthened beams in the experimental dataset.

| Variable | Min | Max | Mean | $Q_1$[1] | Median | $Q_3^2$ | Std[3] | CoV[4] |
|---|---|---|---|---|---|---|---|---|
| Concrete mean compressive strength $f_{cm}$ (MPa) | 10.6 | 61.3 | 33.7 | 27.4 | 32.8 | 38.0 | 10.1 | 0.3 |
| Axial stiffness of FRP $E_f\rho_f$ (N/mm$^2$) | 38.4 | 3339.7 | 494.3 | 190.1 | 340.4 | 593.9 | 457.37 | 0.92 |
| Stirrup ratio $\rho_{sw}$(%) | 0 | 0.84 | 0.164 | 0 | 0.106 | 0.26 | 0.194 | 1.18 |
| Longitudinal steel ratio $\rho_{sl}$(%) | 0.3 | 5.8 | 2.6 | 1.55 | 2.4 | 3.7 | 1.2 | 0.46 |
| Width of the beam's web $b_w$(mm) | 76 | 600 | 180.2 | 122.2 | 150 | 250 | 81.4 | 0.45 |
| Height of the beam's web $h_w$(mm) | 150 | 762 | 341.9 | 252.5 | 305 | 420 | 116.1 | 0.34 |

[1] $Q_1$ lower quartile, [2] $Q_3$ upper quartile, [3]Std standard deviation, and [4]CoV coefficient of variation.

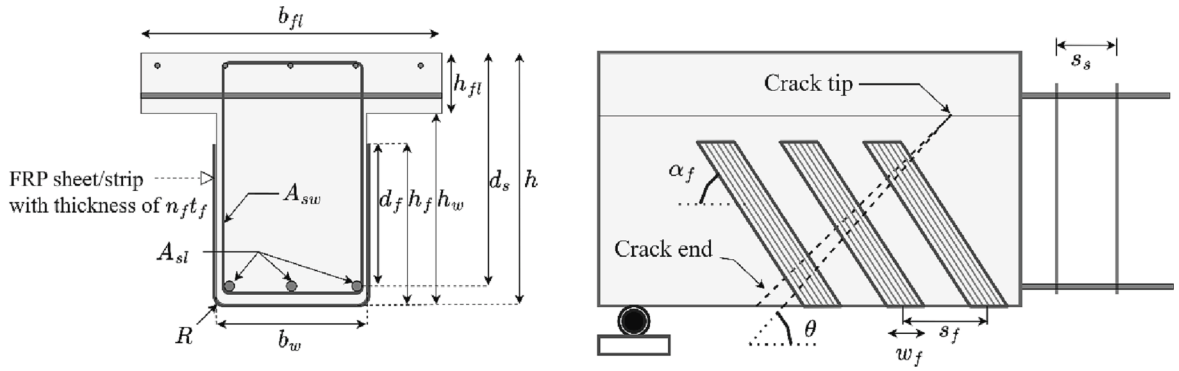


**Fig. 2.** Representation of the physical meaning of the variables adopted in the formulations.

respectively. The effective thickness, $t_{fe}$, is equal to $n_f t_f$ for up to three layers of FRP and is equal to $(n_f t_f)^{0.85}$ for four and more layers ($n_f$ is the number of layers), being $t_f$ the thickness of one layer of FRP. In Eq. (4) $\theta$ is the crack inclination angle, and $f_{fe}$ is the effective strength of FRP, which is governed by either FRP rupture or debonding failure modes. The model assumes that in fully wrapped beams FRP fails by its tensile rupture:

$$f_{fe} = f_{fw,c} = a_t k_R . f_{fu} \tag{5}$$

$$\kappa_R = \begin{cases} 0.5\dfrac{R}{50}\left(2-\dfrac{R}{50}\right) & R < 50\,mm \\ 0.5 & R \geqslant 50\,mm \end{cases} \tag{6}$$

where $\kappa_R$ is a modification factor accounting for the stress gradient due to the effect of rounding the corner of the beam's cross-section with a certain radius ($R$ *in mm*). The $a_t$ in Eq. (5) is a reduction factor to account for the long-term effects (taken equal to 1.0 in this study), and $f_{fu}$ is the value of the tensile rupture of the FRP.

For beams strengthened with U-wrapped FRPs:

$$f_{fe} = \min\left(f_{fw,c}, f_{fbw}\right) \tag{7}$$

where $f_{fbw}$ is the bond strength of shear strengthening system.

For continuous FRP sheets:

$$\text{a)}\ f_{fbw} = \left[1 - \frac{1}{3}\frac{l_e}{\left(h_{fe}/\sin\alpha_f\right)}\right] f_{fbk} \quad for\ x \geqslant l_e \tag{8}$$

$$\text{b)}\ f_{fbw} = \frac{2}{3}\frac{h_{fe}/\sin\alpha_f}{l_e} f_{fbk} \quad for\ x \leqslant l_e \tag{9}$$

For discrete FRP strips:

$$\text{a)} f_{fbw} = f_{fbk} \quad for\ x \geqslant l_e;\ and\ \ l_e \leqslant y \leqslant x \tag{10}$$

$$\text{b)} f_{fbw} = \left[1 - \left(1 - \frac{2}{3}\frac{ms_f}{l_e}\right)\frac{m}{n}\right] f_{fbk} \quad for\ x \geqslant l_e;\ and\ \ y \leqslant l_e \tag{11}$$

$$\text{c)}\ f_{fbw} = \frac{2}{3}\frac{\left(ns_f\right)/\left[\left(\cot\theta + \cot\alpha_f\right)\sin\alpha_f\right]}{l_e} f_{fbk} \quad for\ x \leqslant l_e;\ and\ \ y \leqslant x \tag{12}$$

where $x$ is calculated as $h_{fe}/sin\alpha_f$, $y$ is $s_f/\left(\left(cot\alpha_f + cot\theta\right)sin\alpha_f\right)$, $n$ and $m$ are the integer part of $h_{fe}\left(cot\alpha_f + cot\theta\right)/s_f$, and $l_e(cot\alpha_f + cot\theta)sin\alpha_f/s_f$, respectively. In previous equations $f_{fbk}$ is the characteristic value of the FRP debonding strengthened $l_e$ is the effective bond length of FRP determined from:

$$f_{fbk} = \sqrt{\frac{E_f s_{0k}\tau_{b1k}}{t_{fe}}} \tag{13}$$

$$l_e = \frac{\pi}{2}\sqrt{\frac{E_f t_{fe} s_{0k}}{\tau_{b1k}}} \tag{14}$$

where $E_f$ is the elastic modulus of FRP, $s_{0k}$ and $\tau_{b1k}$ are characteristic ultimate slip and bond strength, respectively.

### 3.2. Cnr-DT 200 R1/2013

The Italian guideline for FRP (CNR-DT 200 R1/2013) [13] has basically adopted and modified the model proposed by Monti and Liotta [20].

$$V_{R,f} = 0.9 d_s . f_{fe} . 2 n_f t_f \left(\cot\theta + \cot\alpha\right)\frac{w_f}{s_f \sin\alpha} \tag{15}$$

The effective strength of FRP is computed according to Eq. (16) for fully wrapped and anchored U-wrapped beams, and Eq. (17) for U-wrapped and side-bonded beams.

$$f_{fe} = f_{fee}\left[1 - \frac{1}{6}\frac{l_e \sin\alpha_f}{\min\{0.9d_s, h_w\}}\right] + \max\left\{0, \left\langle \frac{1}{2}\left(\kappa_R . f_{fu} - f_{fee}\right)\left[1 - \frac{l_e \sin\alpha_f}{\min\{0.9d_s, h_w\}}\right]\right\rangle\right\} \leqslant 0.005 E_f \tag{16}$$

$$f_{fe} = f_{fee}\left[1 - \frac{1}{3}\frac{l_e \sin\alpha}{\min\{0.9d_s, h_w\}}\right] \leqslant 0.005 E_f \tag{17}$$

In the above equations, $\kappa_R$ is a reduction factor due to local stress in

corners, which is obtained by Eq. (18). $l_e$ is the effective bond length computed according to Eq. (22).

$$\kappa_R = 0.2 + 1.6\frac{R}{b_w},\ with\ \ 0 \leqslant \frac{R}{b_w} \leqslant 0.5 \tag{18}$$

$f_{fee}$ is the FRP debonding stress, which is computed according to:

$$f_{fee} = \sqrt{\frac{2E_f\Gamma_{fe}}{n_f t_f}} \tag{19}$$

where

$$\Gamma_{fe} = k_b k_G \sqrt{f_{cm} f_{ctm}} \tag{20}$$

being $k_G$ an empirical coefficient, whose mean value is equal to 0.037 for wet-layup sheets and 0.023 for precured FRP composites, and

$$k_b = 1 \leqslant \sqrt{\frac{2 - w_f/(s_f \sin\alpha_f)}{1 + w_f/(s_f \sin\alpha_f)}} \leqslant 1.18 \tag{21}$$

In Eqs. (14) and (15)

$$l_e = \max\left\{\frac{1}{f_{be}}\sqrt{\frac{\pi^2 E_f n_f t_f \Gamma_{Fe}}{2}}, 200\ \text{mm}\right\} \tag{22}$$

with

$$f_{be} = \frac{2\Gamma_{Fe}}{s_u} \tag{23}$$

In the case of using continuous sheets, $w_f$ is substituted with $min(0.9d, h_w)sin(\alpha_f + \theta)/sin\theta$ , and $s_f$ is substituted with $w_{fv}/sin\alpha_f$. $s_u$ is the ultimate FRP-support slip, taken as 0.25 mm.

### 3.3. Aci 440.2R-17

According to the American Concrete Institute [11] the contribution of a FRP system for the shear strengthening of RC beams is obtained from:

$$V_{R,f} = \frac{2n_f t_f w_f f_{fe} d_f (\sin\alpha_f + \cos\alpha_f)}{s_f} \tag{24}$$

$$f_{fe} = E_f \varepsilon_{fe} \tag{25}$$

where $d_f$ and $\varepsilon_{fe}$ are the effective depth and the effective strain of FRP, which is equal to the minimum of 0.004 and 0.75 $\varepsilon_{fu}$ in case of fully wrapped beams, and is computed according to eq. (26) for U-wrapped beams.

$$\varepsilon_{fe} = \frac{\kappa_1 \kappa_2 L_e}{11900}\varepsilon_{fu} \leqslant \min(0.75\varepsilon_{fu}, 0.004) \tag{26}$$

where $\varepsilon_{fu}$ is the ultimate tensile strain of the FRP, while $\kappa_1$ and $\kappa_2$ parameters are determined from:

$$\kappa_1 = \left(\frac{f_c'}{27}\right)^{2/3} \tag{27}$$

$$\kappa_2 = \frac{d_{fv} - L_e}{d_{fv}} \tag{28}$$

for taking in consideration the quality of the concrete substrate and geometry shear strengthening configuration, respectively, while $L_e$ is the FRP effective bond length:

$$L_e = \frac{23300}{(n_f t_f E_f)^{0.58}} \tag{29}$$

## 4. Proposed model

The proposed model considers the parameters that highly affect the contribution of FRP for the shear strength of a RC element, including the interaction between existing steel stirrups and FRP shear reinforcement. In this study, a truss analogy-based model is adopted, by estimating the effective strain in the FRP reinforcement through a regression-based prediction equation that considers the experimentally FRP shear contribution, $V_f^{exp}$:

$$\varepsilon_{fe} = \frac{V_f^{exp}}{A_{fwc} h_{fe} E_f (1 + \cot\alpha_f)\sin\alpha_f}$$

where $A_{fwc}$ and $h_{fe}$ are as introduced in *fib* bulletin 90. It is assumed the critical diagonal crack has an inclination angle of 45 degrees. Firstly, the correlation between each predictive variable and the effective strain of FRP ($\varepsilon_{fe}$) is explored and reported to comprehend their relationship, Fig. 3. Then, a regression equation accompanied by several modification factors is proposed. As shown, a five-by-five matrix is established, with the figures in its diagonal representing the histogram for the distribution of each variable. The information below and above this diagonal represent the scatter plots and Pearson correlation coefficient, respectively. To emphasize the significance of relationship between the normalized axial stiffness of FRP and effective strain by assistance of linear correlation, the logarithm of $\rho_f E_f / f_{cm}^{2/3}$ is used to convert a nonlinear relation to a linear one. The linear correlation is evaluated using the Pearson correlation coefficient represented by the symbol "r" as depicted in the figure. According to Fig. 3 the effective strain of FRP generally decreases as the axial stiffness of FRP rises which can be justified by the no integral shear strengthening mobilization of the existing steel stirrups with the increase of $E_f\rho_f$. Furthermore, it is recognised that by decrease in the concrete compressive strength lower value of effective strain is obtained. These effects where considered together in the model taking $\rho_f E_f / f_{cm}^{2/3}$ variable. The obtained results show a decrease of in the effective strain of FRP with the increase of the reinforcement ratio of existing steel stirrups ($r = -0.20$). This can be justified by mechanisms contributing for the premature debonding of FRP when the stirrups are spaced in shorter distance, as demonstrated elsewhere [106]. Moreover, as expected from the physical understanding, data generally exhibit higher values of effective strain for the case of fully wrapped specimens ($r = 0.33$). The database however is unable to show the expected behaviour in the case of corner radius where it is physically proven that higher corner radiuses will avoid premature FRP rupture due to stress concentration. This could be attributed to the limited and uncertain information available in the literature regarding the corner radius of the beam's cross-section. Which, consequently, leads to observe no direct positive linear relationship ($r = -0.02$) with the estimated effective strain. Nonetheless, it has been conceptually shown that an increase in this variable would result in a rise in the effective strain [105]. Later, a modification factor will be proposed for this variable by considering this reality.

According to the truss analogy and assuming a crack inclination angle of 45°, Eq. (31) can be proposed for the contribution of FRP in the shear capacity of the beam:

$$V_{R,f} = A_{fwc} h_{fe} E_f \varepsilon_{fe} (1 + \cot\alpha_f)\sin\alpha_f \tag{31}$$

The proposed equation for the effective strain ($\varepsilon_{fe}$) is expressed as follows:

$$\varepsilon_{fe} = m_F \times 0.038 \times \left(E_f \rho_f / f_{cm}^{2/3}\right)^{-0.765} \tag{32}$$

In this equation $m_F$ is the recommended modification factor:

$$m_F = \kappa_{sw}\kappa_R\kappa_{O/U} \tag{33}$$

$$\kappa_{sw} = 1 - 24.1\rho_{sw} \tag{34}$$

$$\kappa_R = 0.17\left(\frac{R}{50}\right) + 0.93 \leqslant 1.1 \tag{35}$$

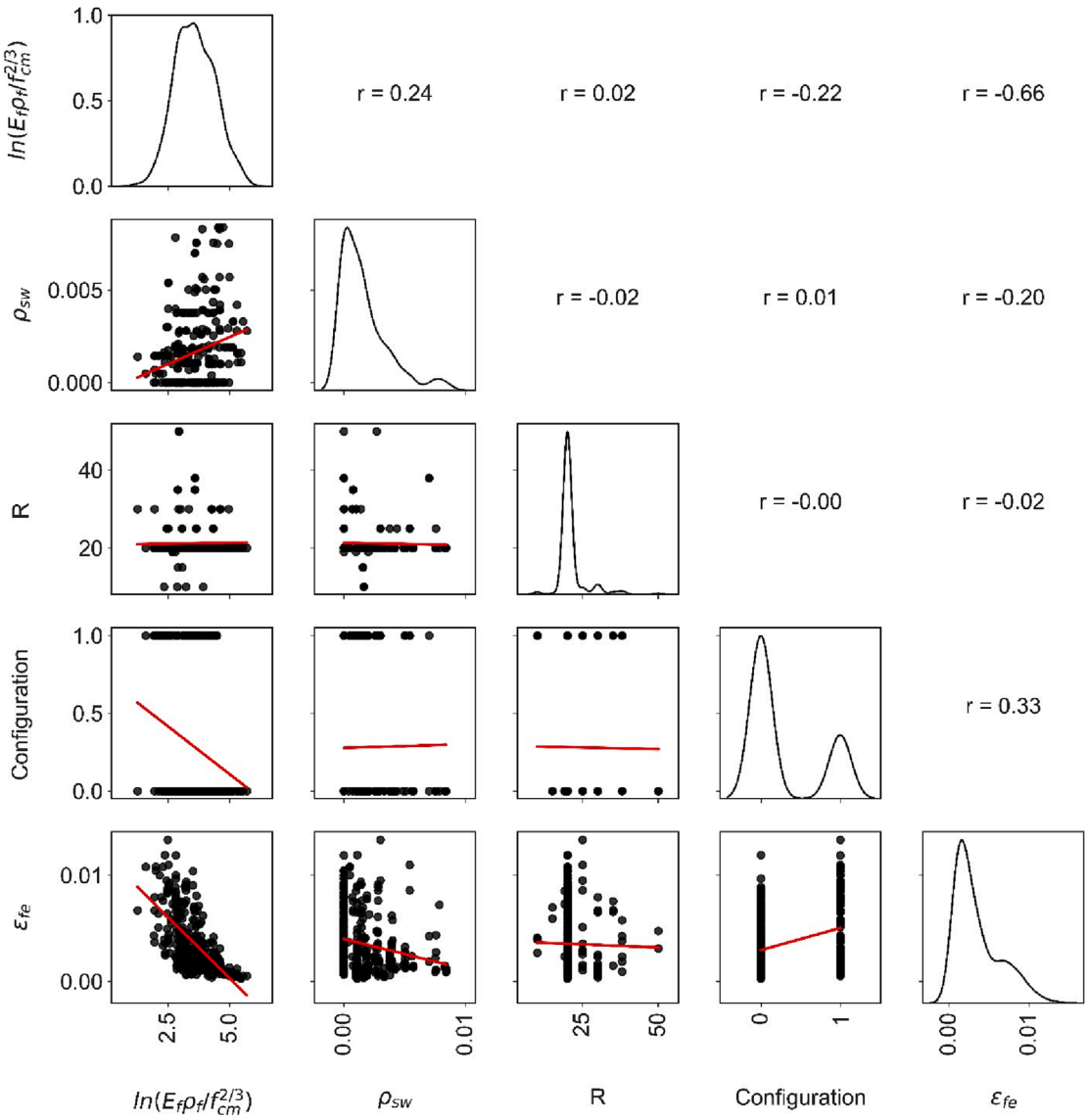


**Fig. 3.** Scatterplots of independent variables and effective strain.

$$\kappa_{O/U} = 0.92 + 0.28\kappa \tag{36}$$

In the above equations, $\kappa_{sw}$ is a modification factor accounting for the interaction between internal steel and external FRP shear reinforcement; $\kappa_R$ is a coefficient for considering the stress concentration in the corners (in which $R$ is Radius at the corner of the beam's cross-section, measured in millimetres); $\kappa_{O/U}$ accounts for the type of FRP shear strengthening configuration; $\rho_{sw}$ is the reinforcement ratio of steel stirrups; $\kappa$ is the strengthening configuration factor, assuming 1.0 and 0 for fully wrapped and U-wrapped beams, respectively.

## 5. Validation and discussion

In this section, the performance of the above described existing design models is compared with the model proposed in this study. For each of the models, the nominal shear contribution of FRP will be computed through the given equations (i.e., $V_{R,f}^{model}$) and then will be compared with the experimental value $V_f^{exp}$. This last term is calculated by subtracting the shear strength of the reference beam, $V_R^{ref}$ from the overall shear strength of the strengthened beam, $V_R^{str}$:

$$V_f^{exp} = V_R^{str} - V_R^{ref} \tag{37}$$

It must be noted that for obtaining the predictions of the models, average values of the material properties are used. The partial and global safety factors and/or long-term modification factors were taken to be equal to 1.0. The inclination of the shear crack is assumed to be 45 degrees (the assumed value in the ACI 440.2R-17 model) to ensure comparable values between all the equations, and also due to the fact this information is generally not provided in the bibliography supporting the database. Whenever the corner radius of the beam's cross-section was not provided, a value of 20 mm was assumed, since it was the average of the available values.

The model uncertainty was evaluated by the ratio between the value recorded experimentally and the predicted one:

$$\chi = \frac{V_{R,f}^{exp}}{V_{R,f}^{model}} \tag{38}$$

Fig. 4 shows the performance of the models in predicting the contribution of FRP for the shear strength of RC beams strengthened with fully wrapped and U-strip configurations. For each model, three columns of plots are provided. The first plot is a representation of $V_{R,f}^{model}$

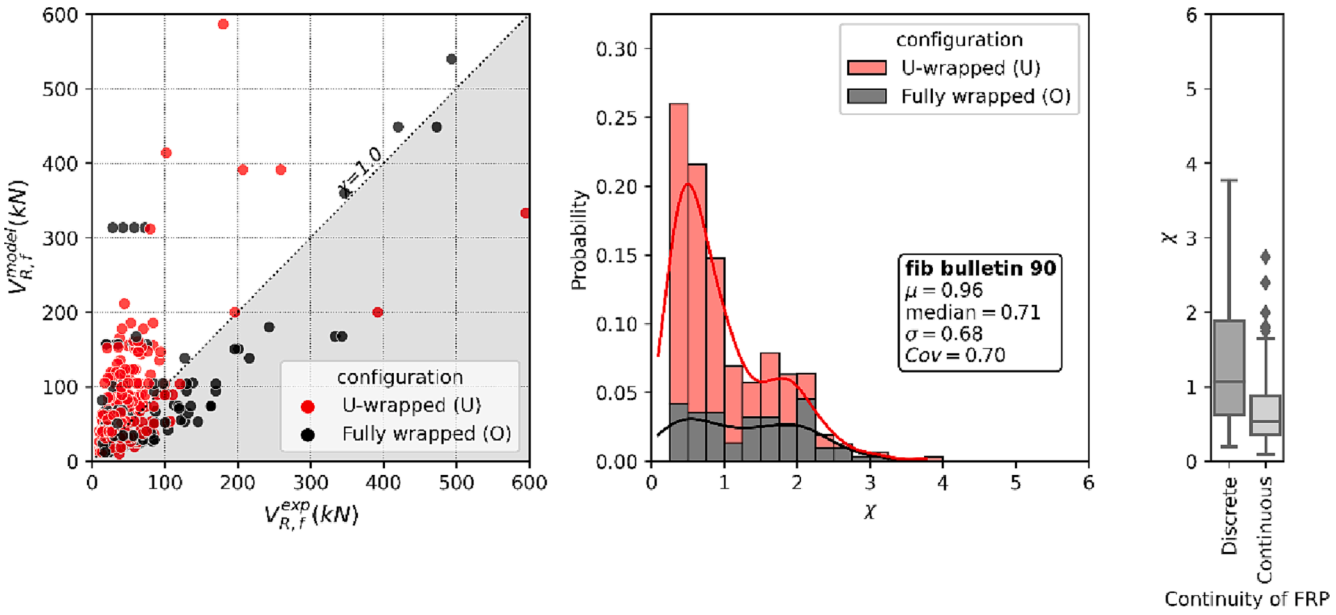


**Fig. 4.** $V_{R,f}^{model}$ *versus* $V_{R,f}^{exp}$(left), distribution of model error probability in entire dataset $\chi$ (middle) and boxplot representation of $\chi$ for continuous and discrete configuration (right) for: (a) *fib* bulletin 90 [12], (b) CNR-DT 200 [13], (c) ACI 440.2R-17 [11], and (d) proposed model.

*versus* $V_{R,f}^{\exp}$. Careful inspection of these figures reveals that the proposed model produces the most straight-line like predictions. The second plot shows the distribution of model error probability for both configurations of strengthened beams (i.e., fully wrapped and U-wrapped). The third plot shows the model error for beams strengthened with continuous FRP sheets and beams strengthened with discrete FRP strips. The mean value ($\mu$), standard deviation ($\sigma$), median, and coefficient of variation (COV) of $\chi$ are reported in Fig. 5.

Fig. 4 reveals that the current models generally result in unconservative responses, which raises serious concerns, despite the safety factors of the models may significantly attenuate the unsafe level of the predictions. The scatter plot of the theoretical *versus* experimental values of shear strength provided by FRP, shows that the prediction models have dispersed results including the proposed model, which may be justified by the difficulty of assuring uniform application methodologies of the strengthening systems, size effects and inadequate loading conditions, since inadequate $a/d$ can avoid the occurrence of a failure due to the formation of a critical diagonal crack. A different percentage of the flexural reinforcement can introduce a distinct profile for the shear failure crack and dowel effect resisting mechanisms, aspects not considered explicitly In major part of the formulations. Fig. 5 shows that of the considered existing models, *fib* bulletin 90 achieved the lowest standard deviation ($\sigma$ = 0.68), however its median value of 0.71 indicates that it tends to give overestimated predictions. ACI 440.2R-17 has the second smallest standard deviation ($\sigma$ = 0.74), but its median (=0.85) indicates a tendency toward overpredictions. CNR-DT200 has the highest standard deviation ($\sigma$ = 0.77), but its median (=0.81) indicates that it also produces unconservative predictions. The proposed model on the other hand, outperforms the considered existing models and produces the lowest standard deviation ($\sigma$ = 0.54). In addition, having a median of 0.92, this model makes less unconservative predictions in comparison with existing models.

The histograms for each model present the probability of model error $\chi$ falling within each interval of 0.25. According to these plots, predictions made by CNR-DT200 and *fib* bulletin 90 are more likely to be overestimated. However, the proposed model shows a better performance for both fully and U-wrapped beams.

The plot in the third column of Fig. 4 shows if the models are biased for beams strengthened with continuous sheets and discrete FRP strips. According to these plots, all considered existing models have more tendency to overestimate beams strengthened with continuous FRP sheets. This may suggest difficulties of assuring proper bond conditions of the FRP to the concrete substrate when using continuous FRP sheets. Fig. 4d shows that unlike other models, the proposed model has unbiased performance for beams reinforced with either FRP strips or continuous FRP sheets.

The performance of models in predicting the shear contribution of FRP is further explored by determining other indicators of accuracy, namely: root mean squared error (RMSE), mean absolute percentage error (MAPE), Absolute Fraction of Variance ($R^2$), and Pearson coefficient of correlation (r):

$$RMSE = \sqrt{\frac{1}{n}\sum_{i=1}^{n}\left(V_{R,f,i}^{mod\ el} - V_{R,f,i}^{\exp}\right)^2} \tag{39}$$

$$MAPE = \frac{100\%}{n}\sum_{i=1}^{n}\left(\frac{\left|V_{R,f,i}^{\text{model}} - V_{R,f,i}^{\exp}\right|}{V_{R,f,i}^{\exp}}\right) \tag{40}$$

$$R^2 = 1 - \frac{\sum_{i=1}^{n}\left(V_{R,f,i}^{mod\ el} - V_{R,f,i}^{\exp}\right)^2}{\sum_{i=1}^{n}\left(V_{R,f,i}^{mod\ el}\right)^2} \tag{41}$$

$$r = \frac{\sum_{i=1}^{n}\left(V_{R,fi}^{\text{model}} - \overline{V_{R,f}^{\text{model}}}\right)\left(V_{R,fi}^{\exp} - \overline{V_{R,f}^{\exp}}\right)}{\sqrt{\sum_{i=1}^{n}\left(V_{R,fi}^{\text{model}} - \overline{V_{R,f}^{\text{model}}}\right)^2\sum_{i=1}^{n}\left(V_{R,fi}^{\exp} - \overline{V_{R,f}^{\exp}}\right)^2}} \tag{42}$$

A model with a perfect prediction has a null value for MAPE and RMSE and the unitary value for r and $R^2$.

The values for these indicators obtained for all models are given in Table 2.

According to Table 2, ACI 440.2R-17 has the highest $R^2$ and *r*, and smaller MAPE and RMSE among the considered existing models. Concerning the proposed model, it has almost a *r* value of 0.8, which means a significant linear correlation between the model predictions and experimental results [107]. The proposed model has also the lowest

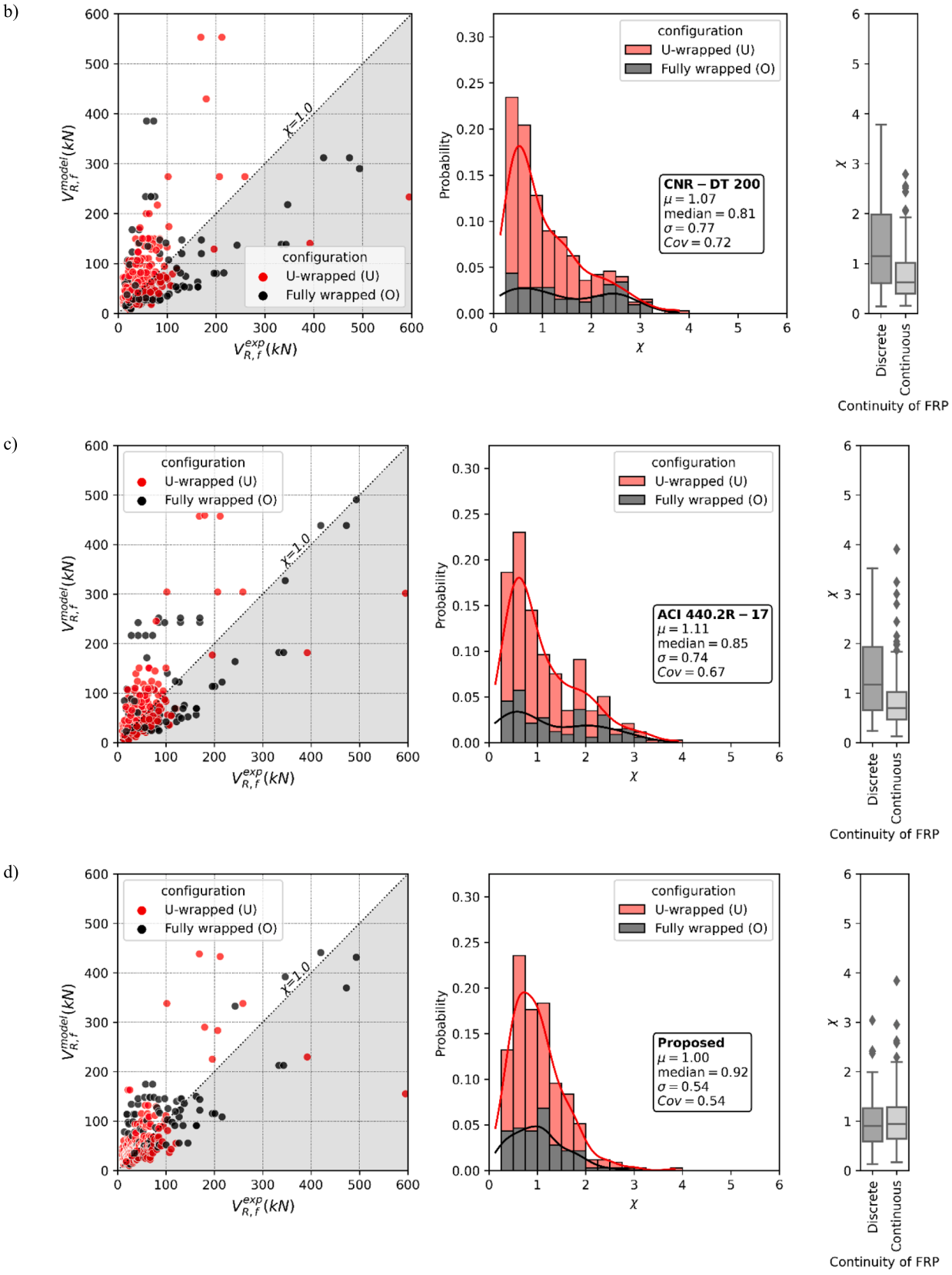


**Fig. 4.** (*continued*).

MAPE and RMSE values, while *fib* bulletin 90 conducted to the largest values.

The considered models, as well as major part of available ones, do not take into consideration the detrimental influence of the percentage of existing steel stirrups on the FRP shear strengthening effectiveness, whose mechanisms are discussed elsewhere [28]. Fig. 6 presents the

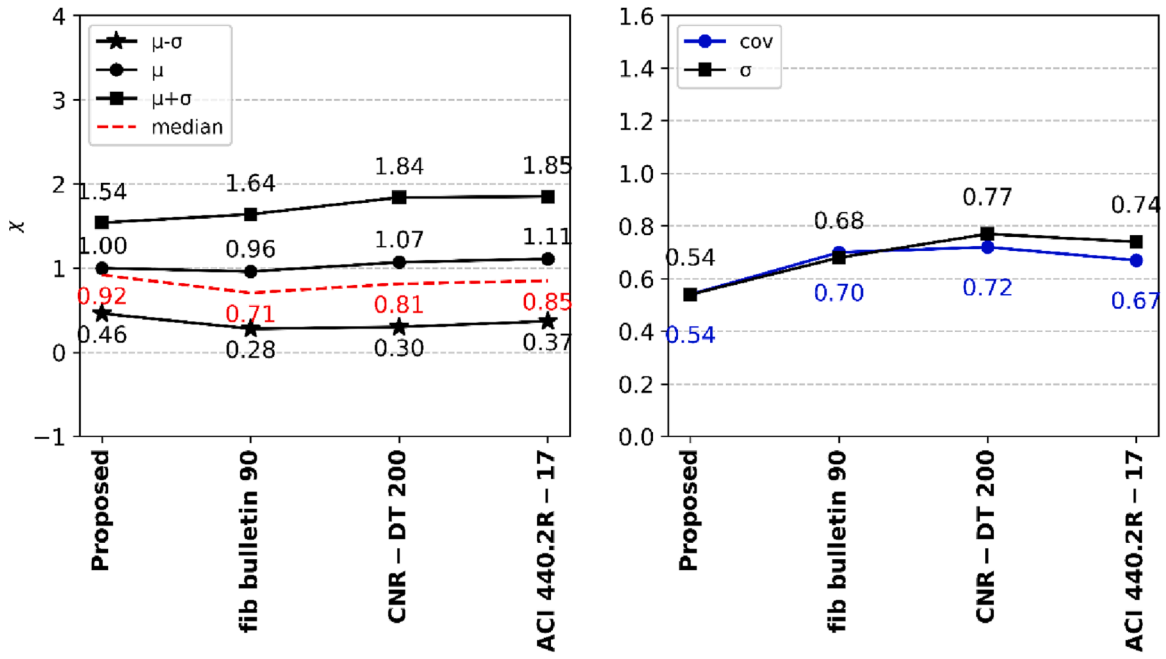


**Fig. 5.** Ratio between the value recorded experimentally and the predicted one ($\chi$) for the different models analysed.

**Table 2**
Prediction performance of the proposed model and the design models.

| Model | RMSE | MAPE (%) | R2 | r |
|---|---|---|---|---|
| *fib* bulletin 90 | 78.1 | 100.4 | 0.63 | 0.63 |
| CNR-DT 200 | 72.7 | 90.4 | 0.52 | 0.53 |
| ACI 440.2R-17 | 59.1 | 74.6 | 0.70 | 0.71 |
| Proposed | 51.4 | 61.8 | 0.74 | 0.76 |

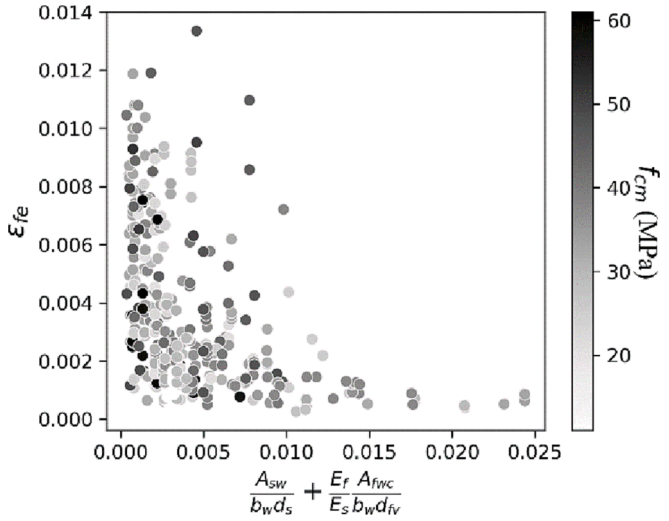


**Fig. 6.** Relation between steel-FRP interaction factor and effective strain in FRP reinforcement.

relation between the steel-FRP interaction factor $(A_{sw}/b_w d_s + (E_f/E_s)A_{fwc}/b_w d_f)$ and the $\chi$ parameter. As can be seen, the effective strain generally decreases as the ratio of steel stirrups or FRP reinforcement increases. This can be justified by the fact that in beams strengthened with a large amount of FRP, the crack opening is restricted, meaning that steel stirrups may fail to reach the yield strain upon failure. Consequently, maximum capacity of steel stirrups is not mobilized and using the yielding stress for their design is incorrect. As a result, it is expected that current models overestimate the results in beams strengthened with a high Steel-FRP interaction factor, since this detrimental effect is not accounted by them. Fig. 7 presents the scatterplot of model errors along the steel-FRP interaction factor and the red line shows the mean of the model error along this factor. *p*-values at a significance level of 0.05 are calculated and displayed to reject or accept the null hypothesis of unbiased estimates. Only in the proposed model with a *p*-value of 0.4, the mean value of the $\chi$ parameter shows no discernible pattern, indicating that the model is not biased with respect to the Steel-FRP interaction factor. In the existing models, the $\chi$ decreases with the increase of the Steel-FRP interaction factor and/or the decrease of the concrete strength. This means that the overpredictions of existing models increase with the Steel- FRP interaction factor and/or the decrease of concrete strength. Therefore, additional considerations should be taken into account when applying these models to beams with a relatively high Steel- FRP interaction factor. As Fig. 7d evidences, this detrimental effect is significantly attenuated in the proposed model, since the percentage of existing steel stirrups, $\rho_{sw}$, is considered via $\kappa_{sw}$ parameter (Eq. (34)).

## 6. Reliability analysis

It should be noted that, from the standpoint of structural reliability, a classification system based solely on the main descriptive statistics measures regarding the behaviour of $\chi$ may not provide enough information to assess the reliability of a design proposal. In fact, a $\chi$ equal to 0.5 is worse than a $\chi$ equal to 2, which is not considered in the statistical analysis provided in the previous section [108]. For this reason, a weighted penalty categorization method, called Demerit Point Scale Methodology, is used [109], where a penalty point is assigned to each range of $\chi$. The total demerit point score for each of the models is obtained by summing the products of the percentage of $\chi$ placing in each range times the demerit points attributed to that range divided by 100. The result of this score will be a number between 0 and 10. The smaller total demerit point score the better the model performs. Table 3 introduces the range of $\chi$ and their penalties, as well as the percentage of specimens that fall within each range. Finally, the overall performance of each model is assessed by a cumulative penalty score. Table 3 shows

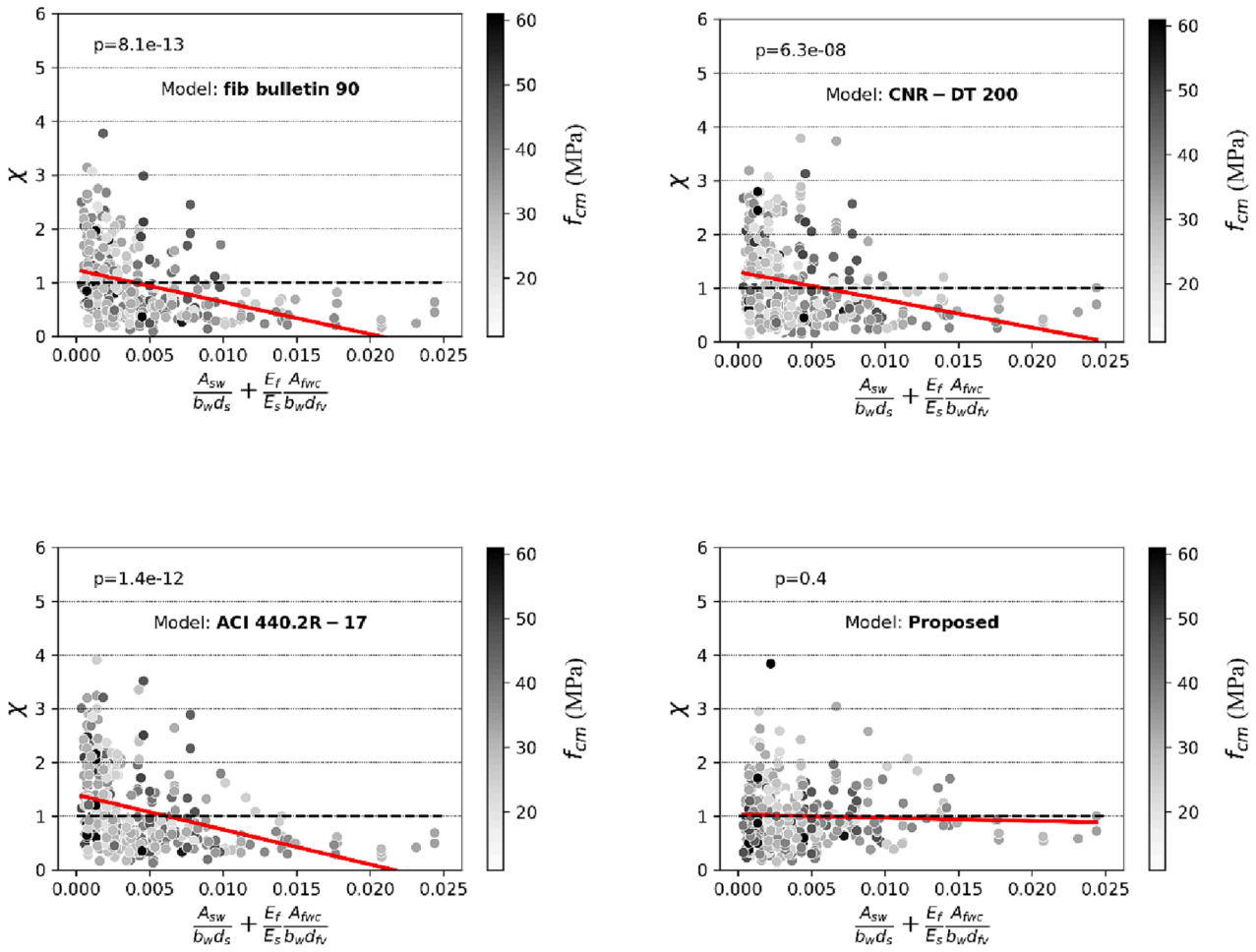


**Fig. 7.** Ratio of experimental to analytical model.

**Table 3**
Demerit point classification.

| χ | Classification | Penalty | *fib* bulletin 90 | CNR-DT 200 | ACI 440.2R-17 | Proposed |
|---|---|---|---|---|---|---|
| <0.5 | Extremely dangerous | 10 | 31 | 27 | 21 | 16[a] |
| 0.5–0.65 | Dangerous | 5 | 15 | 13 | 14 | 13 |
| 0.65–0.85 | Low safety | 2 | 10 | 11 | 16 | 15 |
| 0.85–1.3 | Appropriate safety | 0 | 17 | 18 | 16 | 33 |
| 1.3–2 | Conservative | 1 | 17 | 16 | 19 | 19 |
| >2 | Extremely conservative | 2 | 10 | 15 | 14 | 4 |
| Total demerit point score | | | 4.42 | 4.03 | 3.59 | 2.82[b] |

a: Percentage of specimens with χ laying in the range.
b:$((16 \times 10) + (13 \times 5) + (15 \times 2) + (33 \times 0) + (19 \times 1) + (4 \times 2))/100 = 2.82$

that compared to the considered existing models, the largest percentage of the predictions fall within the appropriate safety range (33% *versus* 17%, 18%, and 16%), while the least percentage of predictions fall inside the dangerous and extremely dangerous ranges (29% *versus* 46%, 40%, and 35%). The total demerit point score of the proposed model is also lower than the considered existing models. Therefore, it is more reliable. The ACI 440.2R-17, with 21% of the predictions in the extremely conservative range, is the most conservative model. On the other hand, 46% of *fib* bulletin 90's predictions fall in dangerous and extremely dangerous ranges, which makes it the less reliable model.

## 7. Conclusions

This paper assessed the performance of some of the most used guideline models for predicting the shear strength of reinforced concrete (RC) beams strengthened with externally bonded fibre reinforced polymer (FRP) reinforcement systems, namely the *fib*-bulletin 90, CNR-DT 200 and ACI 440.2R-17. For this purpose, a comprehensive database formed by results from scrutinized 344 RC beams was set from available literature. In the present phase, the shear strengthening FRP systems of this database are limited to those applied as full wrapping and three-sided (U-wrapped) configurations. In addition, a new model was proposed, and its prediction performance was compared with the above-mentioned existing guideline models. Based on the results and discussions presented in this paper, the following conclusions can be drawn:

1- Among the existing models, ACI 440.2R-17 has the least prediction errors and highest accuracy, supported by the values obtained in RMSE, MAPE, $R^2$ and r, namely, 59.1, 74.6%, 0.70, and 0.71,

respectively, and supported by the $\chi = V_{R,f}^{exp}/V_{R,f}^{model}$ parameter, where $V_{R,f}^{exp}$ and $V_{R,f}^{model}$ are the FRP shear contribution registered experimentally and predicted one by the model, respectively. Nevertheless, it has a high standard deviation ($\sigma = 0.74$), showing that this model has high dispersed prediction errors. The proposed model not only has the best predictive indicators (RMSE = 51.4, MAPE = 61.8, $R^2 = 0.74$ and $r = 0.76$), but also the standard deviation (0.54).

2- None of the current models considers the interaction between the internal steel stirrups and externally bonded FRP reinforcement. Ignoring this effect has contributed to overestimate the shear strengthening capacity of FRP strips, with an increase of the overestimation prediction with the axial stiffness of the FRP system. The proposed model improved this shortcoming of the considered existing models by considering in the formulation a factor that depends on the steel stirrups reinforcement ratio.

3- According to the reliability analysis performed in this study, the proposed model produces the most reliable predictions in comparison with current models. Nevertheless, there is a 29% probability of dangerous and extremely dangerous predictions, which is still a concern that requires further research, mainly to have rational justification.

4- For close future research the authors plan to use the existing database for determining $\chi_d = V_R^{exp}/V_{Rd}^{model}$, where $V_R^{exp}$ and $V_{Rd}^{model} = V_{Rd,c} + V_{Rd,s} + V_{Rd,f} \leqslant V_{Rd,max}$ are beam's shear capacity registered experimentally and predicted by the model, respectively. For the $V_{Rd}^{model}$, the design values of the shear contribution provided by concrete ($V_{Rd,c}$), steel stirrups ($V_{Rd,s}$) and FRP ($V_{Rd,f}$) will be evaluated according to the formulations of the corresponding design guidelines, in order to have a realistic scenario of the $\chi_d$ in real design practice.

## CRediT authorship contribution statement

**Amirhossein Mohammadi:** Conceptualization, Methodology, Formal analysis, Investigation, Visualization, Writing – original draft. **Joaquim A.O. Barros:** Conceptualization, Validation, Supervision, Writing – review & editing. **Jose Sena-Cruz:** Validation, Supervision, Writing – review & editing.

## Declaration of Competing Interest

The authors declare that they have no known competing financial interests or personal relationships that could have appeared to influence the work reported in this paper.

## Data availability

Data will be made available on request.

*Acknowledgements*

This work is financed by national funds through FCT - Foundation for Science and Technology, under grant agreement 2020.08876.BD attributed to the first author. The authors also acknowledge the financial support provided by ANI through the project Sticker – Innovative technique for the structural strengthening based on using CFRP laminates with multifunctional attributes and applied with advanced cement adhesives, with reference POCI-01-0247-FEDER-039755. This work was partly financed by FCT/MCTES through national funds (PIDDAC) under the R&D Unit Institute for Sustainability and Innovation in Structural Engineering (ISISE), under reference UIDB/04029/2020, and under the Associate Laboratory Advanced Production and Intelligent Systems ARISE under reference LA/P/0112/2020.

**Data availability statement.**

All data, models, and code generated or used during the study appear in the submitted article.

## Appendix A. Supplementary material

Supplementary data to this article can be found online at https://doi.org/10.1016/j.compstruct.2023.117081.

## References

[1] Santos GS, Melo GSSA, Barros JAO. Punching CFRP-based strengthening solutions for reinforced concrete flat slabs. Compos Struct 2019;224:111077. https://doi.org/10.1016/j.compstruct.2019.111077.
[2] Almassri B, Barros JAO, al Mahmoud F, Francois R. A FEM-based model to study the behaviour of corroded RC beams shear-repaired by NSM CFRP rods technique. Compos Struct 2015;131:731–41. 10.1016/j.compstruct.2015.06.030.
[3] Almassri B, Kreit A, al Mahmoud F, Francois R. Behaviour of corroded shear-critical reinforced concrete beams repaired with NSM CFRP rods. Compos Struct 2015;123:204–15. 10.1016/j.compstruct.2014.12.043.
[4] Askan A, Gülerce Z, Roumelioti Z, Sotiriadis D, Melis NS, Altindal A, et al. The Samos Island (Aegean Sea) M7.0 earthquake: analysis and engineering implications of strong motion data. Bull Earthq Eng 2021;20:7737–62. https://doi.org/10.1007/s10518-021-01251-5.
[5] Mortezaei A, Ronagh HR, Kheyroddin A. Seismic evaluation of FRP strengthened RC buildings subjected to near-fault ground motions having fling step. Compos Struct 2010;92:1200–11. https://doi.org/10.1016/j.compstruct.2009.10.017.
[6] Altindal A, Karimzadeh S, Erberik MA, Askan A, Anil O, Kockar MK, et al. A case study for probabilistic seismic risk assessment of earthquake-prone old urban centers. Int J Disaster Risk Reduct 2021;61:102376. https://doi.org/10.1016/j.ijdrr.2021.102376.
[7] Dias SJE, Barros JAO. Shear strengthening of RC beams with NSM CFRP laminates: Experimental research and analytical formulation. Compos Struct 2013;99:477–90. https://doi.org/10.1016/j.compstruct.2012.09.026.
[8] Rezazadeh M, Costa I, Barros J. Influence of prestress level on NSM CFRP laminates for the flexural strengthening of RC beams. Compos Struct 2014;116:489–500. https://doi.org/10.1016/j.compstruct.2014.05.043.
[9] Annaiah RH, Myers JJ, Nanni A. Shear Performance of RC BeamsStrengthened In Situ with Composites 2001.
[10] Jiang K, Han Q, Bai Y, Du X. Data-driven ultimate conditions prediction and stress-strain model for FRP-confined concrete. Compos Struct 2020;242:112094. https://doi.org/10.1016/J.COMPSTRUCT.2020.112094.
[11] ACI440.2R-17. Guide for the design and construction of externally bonded FRP systems for strengthening existing structures. 2017.
[12] Struct Concr 2019;10.35789/fib.BULL.0090.
[13] CNR-DT200R1/2013. Guide for the design and construction of externally bonded FRP systems for strengthening existing structures. Roma: CNR – Advisory Committee on Technical Recommendations for Construction; 2013.
[14] Berset JD. Strengthening of reinforced concrete beams for shear using FRP composites. Massachusetts institute of technology 1992.
[15] Vielhaber J, Limberger E. Upgrading of concrete beams with a local lack of shear reinforcement. Germany: Federal Institute for Materials Research and Testing (BAM), Unpublished Report, Berlin; 1995.
[16] Uji K. Improvement of Shear Capacity of Existing Reinforced Concrete Members with Sheet Type Carbon Fibre Reinforcement. Concrete Research and Technology 1992;3:37–47. https://doi.org/10.3151/crt1990.3.2_37.
[17] Triantafillou TC. Shear strengthening of reinforced concrete beams using epoxy-bonded FRP composites. ACI Struct J 1998;95(107–15). pp. 10.14359/531.
[18] Triantafillou TC, Antonopoulos CP. Design of Concrete Flexural Members Strengthened in Shear with FRP. J Compos Constr 2000;4:198–205. https://doi.org/10.1061/(ASCE)1090-0268(2000)4:4(198).
[19] fib bulletin 14. Externally bonded FRP reinforcement for RC structures. vol. 14. 2001.
[20] Monti G, Liotta M. Tests and design equations for FRP-strengthening in shear. Constr Build Mater 2007;21:799–809. https://doi.org/10.1016/j.conbuildmat.2006.06.023.
[21] Matthys S, Triantafillou T. Shear and Torsion Strengthening with Externally Bonded FRP Reinforcement. Composites in Construction 2001:203–12.
[22] Zhang Z, Hsu C-T-T. Shear Strengthening of Reinforced Concrete Beams Using Carbon-Fiber-Reinforced Polymer Laminates. J Compos Constr 2005;9:158–69.
[23] Chen JF, Teng JG. Shear capacity of FRP-strengthened RC beams: FRP debonding. Constr Build Mater 2003;17:27–41. https://doi.org/10.1016/S0950-0618(02)00091-0.
[24] Deniaud C, Cheng JJR. Simplified Shear Design Method for Concrete Beams Strengthened with Fiber Reinforced Polymer Sheets. J Compos Constr 2004;8:425–33. https://doi.org/10.1061/(asce)1090-0268(2004)8:5(425).
[25] Li A, Diagana C, Delmas Y. CRFP contribution to shear capacity of strengthened RC beams. Eng Struct 2001;23:1212–20. https://doi.org/10.1016/S0141-0296(01)00035-9.
[26] Pellegrino C, Modena C. An Experimentally Based Analytical Model For The Shear Capacity Of Frp Strengthened Reinforced Concrete Beams 2008;44:231–45.
[27] Mofidi A, Chaallal O. Shear Strengthening of RC Beams with EB FRP: Influencing Factors and Conceptual Debonding Model. J Compos Constr 2011;15:62–74. https://doi.org/10.1061/(asce)cc.1943-5614.0000153.

[28] Chen GM, Teng JG, Chen JF. Shear Strength Model for FRP-Strengthened RC Beams with Adverse FRP-Steel Interaction. J Compos Constr 2013;17:50–66. https://doi.org/10.1061/(asce)cc.1943-5614.0000313.

[29] Chen GM, Teng JG, Chen JF, Rosenboom OA. Interaction between Steel Stirrups and Shear-Strengthening FRP Strips in RC Beams. J Compos Constr 2010;14: 498–509. https://doi.org/10.1061/(asce)cc.1943-5614.0000120.

[30] Malek AM, Saasatmanesh H. Ultimate shear capacity of reinforced concrete beams strengthened with web-bonded fiber-reinforced plastic plates. Structural Journal, American Concrete Institute, ACI 1998;95:391–9.

[31] Malek AM, Saadatmanesh H. Analytical study of reinforced concrete beams strengthened with web-bonded fiber reinforced plastic plates or fabrics. ACI Struct J 1998;95:343–52.

[32] Deniaud C, Cheng JJR. Review of shear design methods for reinforced concrete beams strengthened with fibre reinforced polymer sheets. Can J Civ Eng 2001;28: 271–81. https://doi.org/10.1139/cjce-28-2-271.

[33] Cao SY, Chen JF, Teng JG, Hao Z, Chen JF. Debonding in RC Beams Shear Strengthened with Complete FRP Wraps. J Compos Constr 2005;9:417–28. https://doi.org/10.1061/(asce)1090-0268(2005)9:5(417).

[34] Vecchio FJ, Collins MP. Modified Compression-Field Theory For Reinforced Concrete Elements Subjected To Shear. Journal of the American Concrete Institute 1986;83(219–31). pp. 10.14359/10416.

[35] Barros JAO, Lima JLT, Meneguetti V, S.J.E. D, Santos LD. Technical report 11-DEC/E-05: DABASUM – Data base for FRP-based shear strengthening of reinforced concrete beams. Guimaraes, Portugal: 2011.

[36] Todeschini R, Ballabio D, Consonni V, Sahigara F, Filzmoser P. Locally centred Mahalanobis distance: A new distance measure with salient features towards outlier detection. Anal Chim Acta 2013;787:1–9. https://doi.org/10.1016/j.aca.2013.04.034.

[37] Sato Y. Ultimate shear capacity of reinforced concrete beams with carbon fiber sheet. Proceedings of Third International Symposium of Non-Metallic (FRP) Reinforcement for Concrete Syructures, vol. 1, 1997, p. 499–506.

[38] SATO Y, Ueda T, KAKUTA Y, Tanaka T. Shear reinforcing effect attached to side of reinforced concrete beams. proceedings of the 2nd international conference on advanced composite materials in bridges and structures, MONTREAL: 1996, p. 621–8.

[39] Araki Matsuzaki Y, Nakano K, Kataoka T, e Fukuyama, H. N. Shear capacity of retrofitted RC members with continuous fiber sheets. Non-Metallic (FRP) Reinforcement for Concrete Structures ,Japan Concrete Institute 1997;1:515–22.

[40] Funakawa Shimono K. Watanabe T. Asada S. e Ushijima S. I. Experimental Study on Shear strenghthening with Continuous Fiber Reinforcement Sheet and Methacrylate Resin. Proceeding of Third International Symposium of Non-Metallic(FRP)Reinforcement for Concrete Strutures 1997;1:475–82.

[41] Kamiharako A, Maruyama K, Takada K, T S. Evaluation of shear contribution of FRP sheets attached to concrete beams. Proceedings of the third international symposium, Non-Metallic FRP reinforcement for concrete structures, Tokyo, Japan: 1997.

[42] ONO K, MATSUMURA M. Strengthening of reinforced concrete bridge piers by carbon fiber sheet. Composite Construction - Conventional and Innovative International Conference (Innsbruck 1997-09-16) 1997:930–1.

[43] Taerwe L, KHALIL H, Matthys S. Behaviour of RC beams strengthened in shear by external CFRP sheets. Proceedings of the Third International Symposium on Non-Metallic (FRP) Reinforcement for Concrete Structures (FRPRCS-3), Sapporo (Japan), 1997, p. 14–6.

[44] Umezu K, Fujita M, Nakai H, e Tamaki K. Shear Behavior of RC Beams with Aramid Fiber Sheet,Japan Concrete Institute,Non-Metallic(FRP) Reinforcement for Concrete Structures. Proceeding of the Third International Symposium 1997; 1:491–8.

[45] Mitsui Y, Murakami K, Takeda K, Sakai H. A study on shear reinforcement of reinforced concrete beams externally bonded with carbon fiber sheets. Compos Interfaces 1997;5:285–95. https://doi.org/10.1163/156855498X00081.

[46] Khalifa A. Shear performance of reinforced concrete beams strengthened with advanced composites 1999.

[47] Christophe D, J. RCJ. Reinforced Concrete T-Beams Strengthened in Shear with Fiber Reinforced Polymer Sheets. Journal of Composites for Construction 2003;7: 302–10. 10.1061/(ASCE)1090-0268(2003)7:4(302).

[48] Park SY, Naaman AE, Lopez MM, Till RD. SHEAR STRENGTHENING EFFECT OF R.C. BEAMS USING GLUED CFRP SHEETS. FRP Composites in Civil Engineering. Proceedings of the International Conference on FRP composites in Civil Engineering, Hong Kong, China: 2001, p. 668–878.

[49] Chaallal O, Hassan M, Shahawy M. Performance of Reinforced Concrete T-Girders Strengthened in Shear with Carbon Fiber-Reinforced Polymer Fabric. ACI Struct J 2002;99. 10.14359/11917.

[50] Barros JAOO, Dias SJEE. Near surface mounted CFRP laminates for shear strengthening of concrete beams. Cem Concr Compos 2006;28:276–92. https://doi.org/10.1016/j.cemconcomp.2005.11.003.

[51] Beber AJ. Comportamento Estrutural de Vigas de Concreto Armado Reforçadas com Compósitos de Fibra de Carbono. Tese (Doutorado Em Engenharia) - Programa de Pós-Graduação Em Engenharia Civil 2003:317.

[52] Diagana C, Li A, Gedalia B, Delmas Y. Shear strengthening effectiveness with CFF strips. Eng Struct 2003;25:507–16. https://doi.org/10.1016/S0141-0296(02)00208-0.

[53] Alagusundaramoorthy P, Harik IE, Choo CC. Shear strength of R/C beams wrapped with CFRP fabric. Kentucky: 2002.

[54] Paul W. Carbon fibre-reinforced polymer plates as shear strengthening for beams. Materials and Structurs 2003;36:291–301.

[55] Zhang Z. Shear strengthening of RC beams using carbon fiber reinforced polymer laminates 2003:178.

[56] Allam SM, Ebeido TI. Retrofitting of RC beams predamaged in shear using CFRP sheets. AEJ - Alexandria Engineering Journal 2003;42:87–101.

[57] Adhikary BB, Ashraf M, Mutsuyoshi H. Shear Strengthening of Reinforced Concrete Beams Using Fiber-Reinforced Polymer Sheets with Bonded Anchorage. ACI Struct J 2004;101(660–8). pp. 10.14359/13388.

[58] Song FX, Fan CZ, Jie L. Experimental research on shear strengthening of reinforde concrete beams with externally bonded CFRP sheets. Southeast University NanJing, China 2004.

[59] Miyajima H, Kosa K, Tasaki K, Matsumoto S. Shear strengthening of RC beams using carbon fiber sheets and its resistance mechanism. Proceedings of the Fifth Workshop on Safety and Stability of Infrastructures against Environmental Impacts, Manila, Philippines: 2005, p. 114–25.

[60] Qu Z, Lu XZ, Ye LP. Size effect of shear contribution of externally bonded FRP U-jackets for RC beams. Proc. International Symposium on Bond Behaviour of FRP in Structures (BBFS 2005), Hong Kong, China, 2005, p. 371–80.

[61] Bousselham A, Chaallal O. Behavior of reinforced concrete T-beams strengthened in shear with carbon fiber-reinforced polymer-an experimental study. ACI Struct J 2006;103:339.

[62] Bousselham A, Chaallal O. Effect of transverse steel and shear span on the performance of RC beams strengthened in shear with CFRP. Compos B Eng 2006; 37:37–46.

[63] Jayaprakash J, Samad AAA, Abbasovich AA, Ali AAA. Shear capacity of precracked and non-precracked reinforced concrete shear beams with externally bonded bi-directional CFRP strips. Constr Build Mater 2008;22:1148–65.

[64] Rizzo A, de Lorenzis L. Behavior and capacity of RC beams strengthened in shear with NSM FRP reinforcement. Constr Build Mater 2009;23:1555–67. https://doi.org/10.1016/j.conbuildmat.2007.08.014.

[65] Grande E, Imbimbo M, Rasulo A. Effect of transverse steel on the response of RC beams strengthened in shear by FRP: Experimental study. J Compos Constr 2009; 13:405–14.

[66] Colalillo MA, Sheikh SA. Seismic retrofit of shear-critical reinforced concrete beams using CFRP. Constr Build Mater 2012;32:99–109.

[67] Ebead U, Saeed H. Hybrid mechanically fastened/externally bonded FRP for RC beam shear strengthening. CICE, Rome, Italy, 2012.

[68] Godat A, Chaallal O. Strut-and-tie method for externally bonded FRP shear-strengthened large-scale RC beams. Compos Struct 2013;99:327–38.

[69] Katakalos K, Manos GC, Papakonstantinou CG. Comparison between carbon and steel fiber reinforced polymers with or without anchorage. 6th CICE, Rome 2012.

[70] Godat A, Qu Z, Lu XZ, Labossiere P, Ye LP, Neale KW. Size effects for reinforced concrete beams strengthened in shear with CFRP strips. J Compos Constr 2010; 14:260–71.

[71] Lee H-K, Cheong SH, Ha S-K, Lee CG. Behavior and performance of RC T-section deep beams externally strengthened in shear with CFRP sheets. Compos Struct 2011;93:911–22.

[72] Mofidi A, Chaallal O, Benmokrane B, Neale KW. Performance and comparison of end-anchorage systems for RC beams strengthened in shear with U wrap FRP. 6th CICE, Rome 2012.

[73] Leung CKY, Chen Z, Lee S, Ng M, Xu M, Tang J. Effect of size on the failure of geometrically similar concrete beams strengthened in shear with FRP strips. J Compos Constr 2007;11:487–96.

[74] Teng JG, Chen GM, Chen JF, Rosenboom OA, Lam L. Behavior of RC beams shear strengthened with bonded or unbonded FRP wraps. J Compos Constr 2009;13: 394–404.

[75] Belarbi A, Murphy M, Bae SW. Shear Strengthening of Full-Scale RC T-Beams with CFRP Sheets. 3rd Asia-Pacific Conference on FRP in Structures, APFIS 2012, 2012.

[76] Manos G, Kourtides V, Matsukas P. Investigation of the flexural and shear capacity of simple R/C beam specimens including repair schemes with fiber reinforced plastics. Proceedings of the eighth international symposium on fibre-reinforced polymer (FRP) reinforcement for concrete structures (FRPRCS-8) University of Patras, Patras, Greece, 2007.

[77] Altin S, Anil Ö, Kopraman Y, Mertoğlu Ç, Kara ME. Improving shear capacity and ductility of shear-deficient RC beams using CFRP strips. J Reinf Plast Compos 2010;29:2975–91.

[78] Bousselham A, Chaallal O. Mechanisms of Shear Resistance of Concrete Beams Strengthened in Shear with Externally Bonded FRP. J Compos Constr 2008;12: 499–512. https://doi.org/10.1061/(asce)1090-0268(2008)12:5(499).

[79] Amir M, Omar C. Shear Strengthening of RC Beams with Externally Bonded FRP Composites: Effect of Strip-Width-to-Strip-Spacing Ratio. J Compos Constr 2011; 15:732–42. https://doi.org/10.1061/(ASCE)CC.1943-5614.0000219.

[80] Grande E, Imbimbo M, Rasulo A. Experimental Response of RC Beams Strengthened in Shear by FRP Sheets. The Open Civil Engineering Journal 2013; 7:127–35. https://doi.org/10.2174/1874149501307010127.

[81] Babu AB, Mutsuyoshi H. Behavior of Concrete Beams Strengthened in Shear with Carbon-Fiber Sheets. J Compos Constr 2004;8:258–64. https://doi.org/10.1061/(asce)1090-0268(2004)8:3(258).

[82] Venkatesha K, Rao K, Dinesh S, Bharatkumar H, Anoop M, Balasubramanian S. Experimental investigation of reinforced concrete beams with and without CFRP wrapping. Slovak Journal of Civil Engineering 2013;20:15–26. https://doi.org/10.2478/v10189-012-0014-7.

[83] Gamino AL. Modelagem física e computacional de estruturas de concreto reforçadas com CFRP. 2007.

[84] Al-Tersawy SH. Effect of fiber parameters and concrete strength on shear behavior of strengthened RC beams. Constr Build Mater 2013;44:15–24. https://doi.org/10.1016/j.conbuildmat.2013.03.007.
[85] Baggio D, Soudki K, Noël M. Strengthening of shear critical RC beams with various FRP systems. Constr Build Mater 2014;66:634–44. https://doi.org/10.1016/j.conbuildmat.2014.05.097.
[86] Farghal OA. Fatigue behavior of RC T-beams strengthened in shear with CFRP sheets. Ain Shams Eng J 2014;5:667–80. https://doi.org/10.1016/j.asej.2014.03.007.
[87] Francesco M, H. AR, Antonio N. Strengthening of Short Shear Span Reinforced Concrete T Joists with Fiber-Reinforced Plasic Composites. Journal of Composites for Construction 2002;6:264–71. 10.1061/(ASCE)1090-0268(2002)6:4(264).
[88] Sim J, Kim G, Park C, Ju M. Shear strengthening effects with varying types of FRP materials and strengthening methods. American Concrete Institute, ACI Special. Publication 2005;SP-230:1665–79.
[89] Ramírez A, Leonard A. Análisis de los modelos de comportamiento de vigas de hormigón armado reforzadas a cortante con polímeros armados con fibras (frp). Validación y calibración experimental 2012.
[90] Bukhari IA, Vollum RL, Ahmad S, Sagaseta J. Shear strengthening of reinforced concrete beams with CFRP. Mag Concr Res 2010;62:65–77. https://doi.org/10.1680/macr.2008.62.1.65.
[91] Qin S, Dirar S, Yang J, Chan AHC, Elshafie M. CFRP Shear Strengthening of Reinforced-Concrete T-Beams with Corroded Shear Links. J Compos Constr 2015;19:4014081. https://doi.org/10.1061/(ASCE)CC.1943-5614.0000548.
[92] Dirar S, Lees JM, Morley CT. Precracked reinforced concrete t-beams repaired in shear with prestressed carbon fiber-reinforced polymer straps. ACI Struct J 2013;110(855–65). pp. 10.14359/51685838.
[93] El-Saikaly G, Chaallal O. Fatigue behavior of RC T-beams strengthened in shear with EB CFRP L-shaped laminates. Compos B Eng 2015;68:100–12. https://doi.org/10.1016/j.compositesb.2014.08.014.
[94] Tetta ZC, Koutas LN, Bournas DA. Textile-reinforced mortar (TRM) versus fiber-reinforced polymers (FRP) in shear strengthening of concrete beams. Compos B Eng 2015;77:338–48. https://doi.org/10.1016/j.compositesb.2015.03.055.
[95] Nguyen-Minh L, Rovňák M. Size effect in uncracked and pre-cracked reinforced concrete beams shear-strengthened with composite jackets. Compos B Eng 2015;78:361–76. https://doi.org/10.1016/j.compositesb.2015.02.035.
[96] El-Maaddawy T, Chekfeh Y. Shear strengthening of t-beams with corroded stirrups using composites. ACI Struct J 2013;110(779–89). pp. 10.14359/51685831.
[97] Dias SJEE, Barros JAOO. Experimental Behaviour of RC Beams Shear Strengthened with NSM CFRP Laminates. Strain 2012;48:88–100. https://doi.org/10.1111/j.1475-1305.2010.00801.x.
[98] Chen GM, Zhang Z, Li YL, Li XQ, Zhou CY. T-section RC beams shear-strengthened with anchored CFRP U-strips. Compos Struct 2016;144:57–79. https://doi.org/10.1016/j.compstruct.2016.02.033.
[99] Frederick FFR, Sharma UK, Gupta VK. Influence of end anchorage on shear strengthening of reinforced concrete beams using CFRP composites. Curr Sci 2017;112(973–81). pp. 10.18520/cs/v112/i05/973-981.
[100] Mhanna HH, Hawileh RA, Abdalla JA. Shear strengthening of reinforced concrete beams using CFRP wraps. Procedia Struct Integrity 2019;17:214–21. https://doi.org/10.1016/j.prostr.2019.08.029.
[101] Cheng CD and JJR. Shear Behavior of Reinforced Concrete T-Beams with Externally Bonded Fiber-Reinforced Polymer Sheets. ACI Struct J 2001;98:386–94. 10.14359/10227.
[102] Rousakis TC, Saridaki ME, Mavrothalassitou SA, Hui D. Utilization of hybrid approach towards advanced database of concrete beams strengthened in shear with FRPs. Compos B Eng 2016;85:315–35. https://doi.org/10.1016/j.compositesb.2015.09.031.
[103] Pellegrino C, Vasic M. Assessment of design procedures for the use of externally bonded FRP composites in shear strengthening of reinforced concrete beams. Compos B Eng 2013;45:727–41. https://doi.org/10.1016/j.compositesb.2012.07.039.
[104] Oller E, Kotynia R, Marí A. Assessment of the existing models to evaluate the shear strength contribution of externally bonded frp shear reinforcements. Compos Struct 2021;266:113641. https://doi.org/10.1016/j.compstruct.2021.113641.
[105] D'Antino T, Triantafillou TC. Accuracy of design-oriented formulations for evaluating the flexural and shear capacities of FRP-strengthened RC beams. Struct Concr 2016;17:425–42. https://doi.org/10.1002/suco.201500066.
[106] Bianco V, Barros JAO, Monti G. Three dimensional mechanical model for simulating the NSM FRP strips shear strength contribution to RC beams. Eng Struct 2009;31:815–26. https://doi.org/10.1016/j.engstruct.2008.12.017.
[107] Smith GN. Probability and statistics in civil engineering. Collins Professional and Technical Books 1986;244.
[108] Barros JAO, Dias SJE, Lima JLT. Efficacy of CFRP-based techniques for the flexural and shear strengthening of concrete beams. Cem Concr Compos 2007;29:203–17. https://doi.org/10.1016/j.cemconcomp.2006.09.001.
[109] Collins MP. Evaluation of shear design procedures for concrete structures. A Report Prepared for the CSA Technical Committee on Reinforced Concrete Design; 2001.
[110] Manos GC, Matsukas PKv. Investigation of the flexural and shear capacity of simple R/C beam specimens including repair schemes with fiber reinforced plastics. In: Proceedings of the eighth international symposium on fibre-reinforced polymer (FRP) reinforcement for concrete structures (FRPRCS-8) University of Patras, Patras, Greece; 2007.
[111] Alrousan MA, R.Z. e I. Size effect of reinforced concrete beams on shear contribution of CFRP composites. In: 9th International symposium on fiber-reinforced polymers reinforcement for concrete structures (FRPRCS-9), Sydney, Australia; 2009.